Reappraisal of the Fluxional Behavior of $Ru_3(\mu\text{-}H)(\mu_3\text{-}\eta^2\text{-}C{\equiv}C^tBu)(CO)_9$ and Evidence for the Concerted Rotation of the $Ru(CO)_2(PMe_2Ph)$ Group in the Enantiomerization of $Ru_3(\mu\text{-}H)(\mu_3\text{-}\eta^2\text{-}C{\equiv}C^tBu)(CO)_8(PMe_2Ph)$

Louis J. Farrugia* and Shirley E. Rae

Department of Chemistry, The University, Glasgow G12 8QQ, Scotland, U.K.

Received May 28, 1991

The fluxional behavior of the alkynyl cluster $Ru_3(\mu\text{-}H)(\mu_3\text{-}\eta^2\text{-}C{\equiv}C^tBu)(CO)_9$ (1) has been reinvestigated by variable-temperature ^{13}C NMR spectroscopy and also by 2D EXSY and 1D magnetization transfer experiments. Three processes have been established. The lowest energy process is a tripodal rotation of the unique $Ru(CO)_3$ group, with $\Delta G^{\ddagger} = 59.1$ kJ mol^{-1}. Two further higher energy processes result in complete carbonyl scrambling without intermetallic CO migration: (i) the rotation of the alkynyl ligand around the metal triangle coupled with hydride migration, $\Delta G^{\ddagger} = 67.0$ kJ mol^{-1}, and (ii) a tripodal rotation in the two equivalent $Ru(CO)_3$ groups, $\Delta G^{\ddagger} = 72.0$ kJ mol^{-1}. The derivative $Ru_3(\mu\text{-}H)(\mu_3\text{-}\eta^2\text{-}C{\equiv}C^tBu)(CO)_8(PMe_2Ph)$ (2) has been prepared and the fluxional behavior examined. Crystal data for 2: monoclinic, space group $P2_1/n$, $a = 10.1257$ (7) Å, $b = 21.432$ (2) Å $c = 12.440$ (1) Å, $\beta = 90.448$ (6)°, $V = 2699.6$ (4) Å^3, R (R_w) = 0.028 (0.039) for 4189 independent, absorption-corrected data. The PMe_2Ph ligand substitutes in an equatorial position on the unique $Ru(CO)_3$ group. Three isomers exist in solution, the major one corresponding to the crystal structure. Exchange within the $Ru(CO)_2(PMe_2Ph)$ group in this isomer occurs as a concerted rotation, resulting in cluster enantiomerization, with $\Delta H^{\ddagger} = 57.3$ kJ mol^{-1} and $\Delta S^{\ddagger} = 35.0$ J mol^{-1} K^{-1}.

Introduction

The fluxional behavior of hydrocarbyl ligands in metal clusters has been intensively studied, since such information may be relevant to the mobility of small organic molecules on metal surfaces.[1] For instance there have been numerous reports on the fluxionality of σ,π-alkynes[2,3] in trinuclear clusters, as well as dynamic NMR studies on clusters containing σ,π-vinyl,[4] -vinylidene,[5] and -allenyl[6] ligands.

In an early study in 1975, Aime et al.[7] reported the carbonyl fluxionality in the σ,π-alkynyl cluster $Ru_3(\mu\text{-}H)(\mu_3\text{-}\eta^2\text{-}C{\equiv}C^tBu)(CO)_9$ (1). This work showed that the lowest energy process was a tripodal rotation of the unique $Ru(CO)_3$ group, σ-bonded to the alkynyl ligand. The activation barrier $\Delta G^{\ddagger}$ was not given in the original report[7] but has since been variously reported as 55.2 (±2.1)[8,9] or 46 (±1)[10] kJ mol^{-1}. At the ^{13}C operating frequency of 25.1 MHz, the two resonances for this group collapse at around 310 K. On further warming, the remaining resonances broaden and collapse, and finally at 426 K a single resonance is observed. These last observations were interpreted as a tripodal rotation in the two equivalent $Ru(CO)_3$ groups, with a $\Delta G^{\ddagger}$ reported as 65.3 (±2.1)[8,9] or 62.7 (±1)[10] kJ mol^{-1}, followed by the onset of total CO exchange.

Chart I

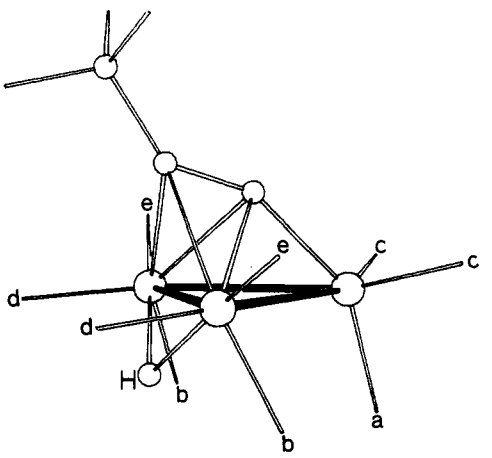

The fluxional behavior of several derivatives of 1 were subsequently reported by the same authors, including $[Ru_3(\mu_3\text{-}\eta^2\text{-}C{\equiv}C^tBu)(CO)_9]^-$[8] and $Ru_3(\mu\text{-}H)(\mu_3\text{-}\eta^2\text{-}C{\equiv}$

(1) (a) Johnson, B. F. G.; Benfield, R. E. In *Transition Metal Clusters*; Johnson, B. F. G., Ed.; Wiley: Chichester, England, 1980; pp 471-543. (b) Band, E.; Muetterties, E. L. *Chem. Rev.* **1978**, *78*, 639.

(2) Raithby, P. R.; Rosales, M. J. *Adv. Inorg. Chem. Radiochem.* **1985**, *29*, 170.

(3) (a) Halet, J.-F.; Saillard, J.-Y.; Lissillour, R.; McGlinchey, M. J.; Jaouen, G. *Inorg. Chem.* **1985**, *24*, 218. (b) Mlekuz, M.; Bougeard, P.; Sayer, B. G.; Peng, S.; McGlinchey, M. J.; Marinetti, A.; Saillard, J.-Y.; Naceur, J. B.; Mentzen, B.; Jaouen, G. *Organometallics* **1985**, *4*, 1123. (c) Busetto, L.; Green, M.; Hessner, B.; Howard, J. A. K.; Jeffery, J. C.; Stone, F. G. A. *J. Chem. Soc., Dalton Trans.* **1983**, 519. (d) Aime, S.; Bertoncello, R.; Busetti, V.; Gobetto, R.; Granozzi, G.; Osella, D. *Inorg. Chem.* **1986**, *25*, 4004. (e) Einstein, F. W. B.; Tyers, K. G. F.; Tracey, A. S.; Sutton, D. *Inorg. Chem.* **1986**, *25*, 1631. (f) Rosenberg, E.; Bracker-Novak, J.; Gellert, R. W.; Aime, S.; Gobetto, R.; Osella, D. *J. Organomet. Chem.* **1989**, *365*, 163. (g) D'Agostino, M. F.; McGlinchey, M. J. *Polyhedron* **1988**, *7*, 807. (h) Bracker-Novak, J.; Hajela, S.; Lord, M.; Zhang, M.; Rosenberg, E.; Gobetto, R.; Milone, L.; Osella, D. *Organometallics* **1990**, *9*, 1379. (i) Gallop, M. A.; Johnson, B. F. G.; Khattar, R.; Lewis, J.; Raithby, P. R. *J. Organomet. Chem.* **1990**, *386*, 121.

(4) (a) Clauss, A. D.; Tachikawa, M.; Shapley, J. R.; Pierpont, C. G. *Inorg. Chem.* **1981**, *20*, 1533. (b) Aime, S.; Gobetto, R.; Osella, D.; Milone, L.; Rosenberg, E.; Anslyn, E. V. *Inorg. Chim. Acta* **1986**, *111*, 95. (c) Bassner, S.; Morrison, E. D.; Geoffroy, G. L. *Organometallics* **1987**, *6*, 2207. (d) Deeming, A. J.; Felix, M. S. B.; Nuel, D.; Powell, N. I.; Tocher, D. A.; Hardcastle, K. I. *J. Organomet. Chem.* **1990**, *384*, 181.

(5) (a) Edidin, R. T.; Norton, J. R.; Mislow, K. *Organometallics* **1982**, *1*, 561. (b) Koridze, A. A.; Kizas, O. A.; Kolobova, N. E.; Petrovskii, P. V.; Fedin, E. I. *J. Organomet. Chem.* **1984**, *265*, C33. (c) Boyar, E.; Deeming, A. J.; Felix, M. S. B.; Kabir, S. E.; Adatia, T.; Bhusate, R.; McPartlin, M.; Powell, H. R. *J. Chem. Soc., Dalton Trans.* **1989**, 5. (d) Grist, N. J.; Hogarth, G.; Knox, S. A. R.; Lloyd, B. R.; Morton, D. A. V.; Orpen, A. G. *J. Chem. Soc., Chem. Commun.* **1988**, 673.

(6) Aime, S.; Gobetto, R.; Osella, D.; Milone, L.; Rosenberg, E. *Organometallics* **1982**, *1*, 640.

(7) Aime, S.; Gambino, O.; Milone, L.; Sappa, E.; Rosenberg, E. *Inorg. Chim. Acta* **1975**, *15*, 53.

(8) Barner-Thorsen, C.; Hardcastle, K. I.; Rosenberg, E.; Siegel, J.; Landfredi, A. M. M.; Tiripicchio, A.; Tiripicchio-Camellini, M. *Inorg. Chem.* **1981**, *20*, 4306.

(9) Jangala, C.; Rosenberg, E.; Skinner, D.; Aime, S.; Milone, L. *Inorg. Chem.* **1980**, *19*, 1571.

(10) Rosenberg, E. *Polyhedron* **1989**, *8*, 383.

0276-7333/92/2311-0196$03.00/0

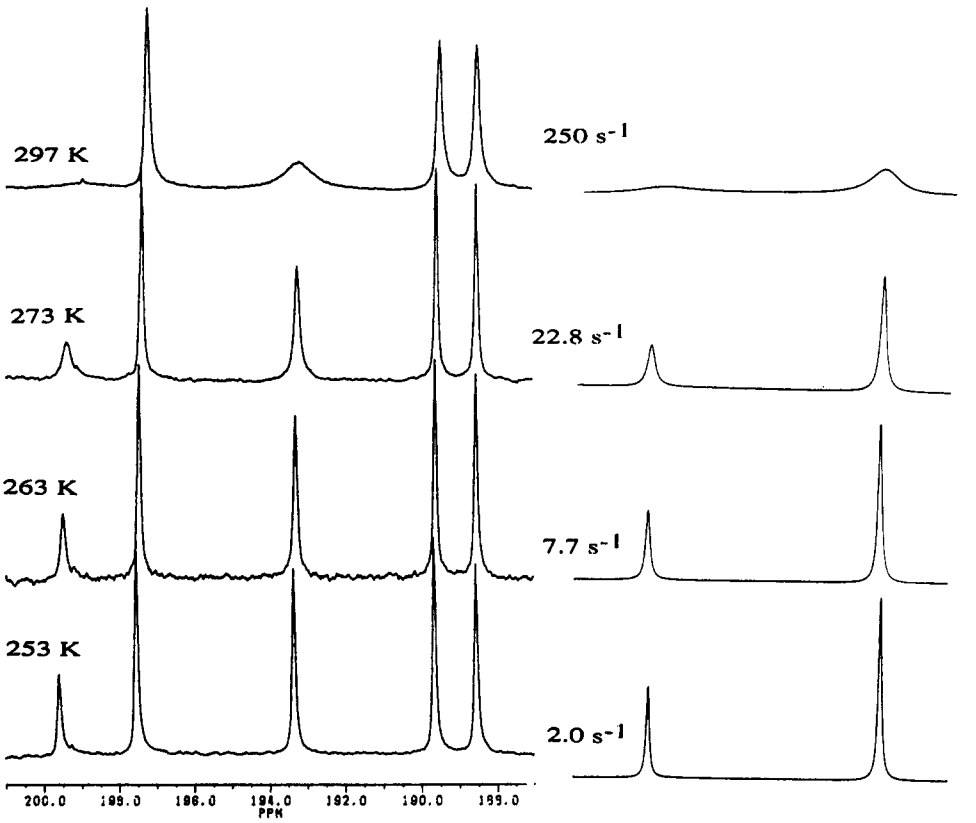

Figure 1. Observed and simulated (resonances a and c only) variable-temperature $^{13}C\{^1H\}$ NMR spectra of **1** in the carbonyl region.

$C^tBu)(CO)_8(L)$ (L = PPh_3,[9] PMePhBz[11]), and these have broadly similar variable-temperature ^{13}C NMR spectra. While these authors[7,8,12] considered that the complete scrambling of CO ligands was most likely to occur via bridged CO intermediates, the possibility of rotation of the alkynyl ligand was also mooted.[13] More recent work by Predieri et al[14a] on the dppm derivative of **1** and Chi et al.[15] on related trinuclear σ,π-alkynyl clusters has demonstrated that alkynyl rotation does occur. Following our own interest[16,17] in the fluxionality of clusters derived from **1**, we have undertaken a reexamination of the dynamic behavior of **1** and shown that the original interpretation is incorrect. We also report herein an examination of the fluxionality of the phosphine derivative $Ru_3(\mu\text{-H})(\mu_3\text{-}\eta^2\text{-}C{\equiv}C^tBu)(CO)_8(PMe_2Ph)$ (**2**).

Results and Discussion

Fluxional Behavior of 1. The variable-temperature $^{13}C\{^1H\}$ NMR spectrum of **1** is shown in Figure 1. The five signals (253 K) at δ 199.4, 197.4 ($^2J_{CH}$ = 3.9 Hz), 193.3, 189.6 ($^2J_{CH}$ = 3.6 Hz), and 188.5 ($^2J_{CH}$ = 14.0 Hz) (referred herein as resonances a–e, respectively) are ca. 3 ppm to high frequency of those reported earlier[8] in the same solvent. Their intensity ratio 1:2:2:2:2 is entirely consistent with the C_s symmetry determined from a neutron diffraction study.[18] Secure assignments to individual carbonyls (Chart I), which are vital for a correct interpretation of any fluxional behavior, were made on the following basis. The signals a and c show no coupling to the hydride and in view of their intensities and exchange behavior are unambiguously assigned to the carbonyls in the unique $Ru(CO)_3$ group. Since resonance e shows the largest coupling to the hydride, it is assigned to the carbonyls trans to this ligand. The couplings to the hydride do not allow a distinction between b and d, although on the basis of chemical shift arguments,[7] the pseudoaxial carbonyl was assigned to resonance b, and the equatorial carbonyl to resonance d. In view of the intrinsic unreliability of such chemical shift correlations, we have carried out a $^{13}C\{^1H\}$ NOE difference experiment to assist in the assignments of b and d. Irradiation at the ^{t}Bu proton frequency resulted in nuclear Overhauser enhancements at all sites, but the enhancement at site b was 43% of the enhancement at site d. This confirms the original assignment of Aime et al.,[7] since the shortest C–H internuclear distances from the ^{t}Bu hydrogens to the carbonyls are 2.74 Å for d and 5.25 Å for b.[18]

The exchange between a and c could be simulated satisfactorily using the exchange rate constants k_{ac}[19] given in Figure 1. From the temperature dependence of k_{ac} we estimate $\Delta H^\ddagger$ = 66.2 (±1.9) kJ mol^{-1} and $\Delta S^\ddagger$ = 24.5 (±7.2) J mol^{-1} K^{-1}. Our value for $\Delta G^\ddagger$ at 275 K of 59.1 (±0.5) kJ mol^{-1} is slightly higher than previously reported.[8-10] It is important to note that, above 273 K, the resonances d and e broaden faster than b; hence, this broadening *cannot* be due simply to a tripodal rotation of the corresponding $Ru(CO)_3$ groups. It is not possible to simulate satisfactorily

(11) Rosenberg, E.; Barner-Thorsen, C.; Milone, L.; Aime, S. *Inorg. Chem.* **1985**, *24*, 231.
(12) Aime, S. *Inorg. Chim. Acta* **1982**, *62*, 51.
(13) See footnote 11 in ref 9.
(14) (a) Predieri, G.; Tiripicchio, A.; Vignali, C.; Sappa, E. *J. Organomet. Chem.* **1988**, *342*, C33. (b) Sappa, E.; Predieri, G.; Tiripicchio, A.; Vignali, C. *J. Organomet. Chem.* **1984**, *378*, 109.
(15) (a) Chi, Y.; Liu, B.-J.; Lee, G.-H.; Peng, S.-H. *Polyhedron* **1989**, *8*, 2003. (b) Hwang, D.-K.; Chi, Y.; Peng, S.-M.; Lee, G.-H. *Organometallics* **1990**, *9*, 2709.
(16) Ewing, P.; Farrugia, L. J. *Organometallics* **1989**, *8*, 1246.
(17) Farrugia, L. J. *Organometallics* **1990**, *9*, 105.
(18) Catti, M.; Gervasio, G.; Mason, S. A. *J. Chem. Soc., Dalton Trans.* **1977**, 2260.
(19) The notation k_{ac} indicates the exchange rate constant *from* site a *to* site c.

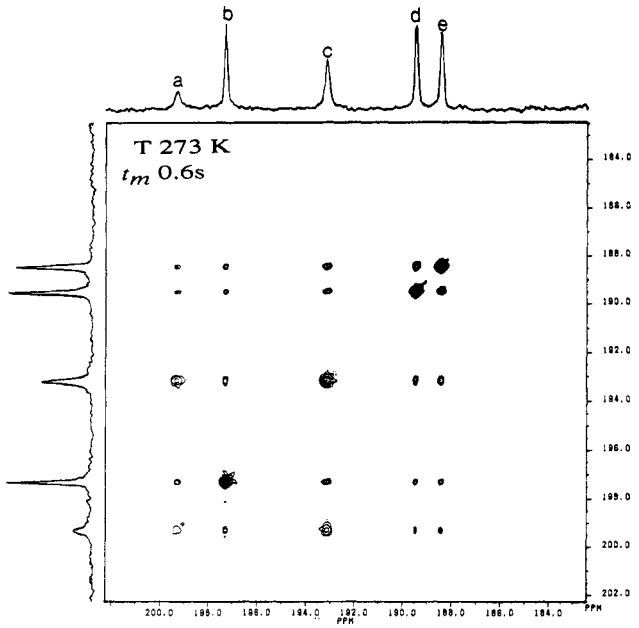

Figure 2. $^{13}C\{^1H\}$ EXSY spectrum of 1 at 273 K in the carbonyl region.

the line broadening of these signals using a single rate constant, as was claimed by Rosenberg et al.[20] We shall return to this point later.

2D EXSY Studies on 1. While the line broadening of NMR signals undergoing chemical exchange gives us information about the rate at which magnetization leaves particular sites, it does not usually provide information as to where that magnetization migrates in a multisite exchange. The 2D NMR technique EXSY produces a graphic display of the multisite exchange matrix.[21-23] The $^{13}C\{^1H\}$ EXSY spectrum of 1 recorded at 273 K, and with a mixing time (t_m) of 0.6 s, is shown in Figure 2. Several important *qualitative* features are evident: (a) Magnetization transfer is observed from all sites to all other sites, confirming complete CO scrambling. However, it does *not* indicate that there is necessarily a *direct* exchange between all sites. (b) The intensity of the cross peak between d and e (I_{de}) is greater than I_{bd} or I_{be}, confirming that d and e exchange with each other faster than they do with resonance b. (c) I_{ad} and I_{ae} are approximately equal to each other, as is also the case for $I_{bd} \approx I_{be}$ and $I_{cd} \approx I_{ce}$, suggesting similar or identical values for the corresponding rate constants, i.e. $k_{ad} \approx k_{ae}$, etc. Any mechanistic interpretation must take these observations into account. It is important to issue a caveat here. While, in the initial rate approximation, the intensities of cross peaks are directly proportional to the site-to-site exchange rate constants,[23] this does not hold true for long mixing times, where second-order components may also contribute intensity.

It is now well established that all site-to-site exchange rate constants may be obtained, in a noniterative fashion, from the integrated volume intensities of a single EXSY spectrum.[21-24] However, the accuracy of such an analysis depends critically on the use of an optimum mixing

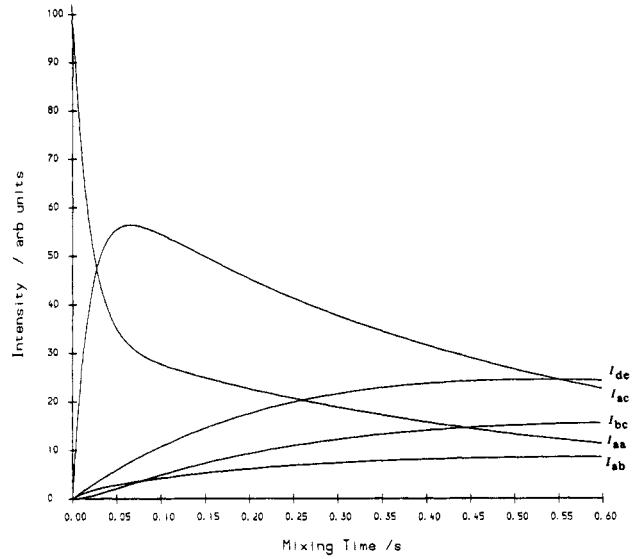

Figure 3. Calculated dependence of selected EXSY intensities on t_m for 1 at 273 K.

Table I. Site-to-Site Exchange Rate Constants (s^{-1}) from the EXSY Spectrum of 1 at 275 K

	$k_{ij}^{a,b}$			
a	b	c	d	e
a	0.94 (±0.5)	26.8 (±7.0)	0.17 (±0.6)	0.17 (±0.6)
b		0.35 (±0.2)	0.09 (±0.08)	0.09 (±0.09)
c			0.48 (±0.25)	0.48 (±0.25)
d				0.92 (±0.18)

[a] $k_{ai} = 2k_{ia}$ due to population differences. [b] Estimated error in parentheses.

time.[23,24] An estimation of optimal values for t_m has been given by Perrin,[25] but unfortunately, in the system under investigation, there is no value of t_m for which an accurate evaluation of all rate constants can be made.

Kinetic analyses on EXSY spectra measured at 275 K,[26] and with t_m values of 0.2, 0.5, and 0.6 s, were carried out according to the method of Abel et al.[24] These gave widely differing rate constants, with large errors. The reason for these problems is readily appreciated from Figure 3, which shows the calculated dependency of the intensities of selected EXSY peaks on t_m. The exchange rate constants used in these calculations were derived from our DANTE studies (see below). With mixing times longer than about 0.05 s I_{aa} and I_{ac} become relatively insensitive to t_m, and the calculated rate constant k_{ac} becomes subject to large errors. The optimal value[25] of t_m for measurement of k_{ac} is about 0.02 s, but then the other cross peaks have intensities of only a few per cent of that of the weakest diagonal peak I_{aa}, and a multisite analysis becomes inherently unreliable. An EXSY spectrum using this mixing time showed only two cross peaks, a strong one between resonances a and c and a weak one between d and e. Kinetic analysis gave a value of 33.1 (±1.7) s^{-1} for k_{ac}, which is identical to that obtained from the DANTE experiments and is consistent with the results of band shape analysis. The results of a kinetic analysis on an EXSY spectrum with t_m of 0.1 s, about the best compromise value, are given in Table I. Since the uncertainties in the site-to-site rate constants precluded any mechanistic interpretation, we

(20) Rosenberg, E.; Anslyn, E. V.; Barner-Thorsen, C.; Aime, S.; Osella, D.; Gobetto, R.; Milone, L. *Organometallics* **1984**, *3*, 1790.
(21) Willem, R. *Prog. Nucl. Magn. Reson. Spectrosc.* **1987**, *20*, 1.
(22) Orrell, K. G.; Sik, V.; Stephenson, D. *Prog. Nucl. Magn. Reson. Spectrosc.* **1990**, *22*, 141.
(23) Perrin, C. L.; Dwyer, T. J. *Chem. Rev.* **1990**, *90*, 935.
(24) Abel, E. W.; Coston, T. P. J.; Orrell, K. G.; Sik, V.; Stephenson, D. *J. Magn. Reson.* **1986**, *70*, 34.
(25) Perrin, C. L. *J. Magn. Reson.* **1989**, *82*, 619.
(26) This temperature was chosen since resonances a and c were still relatively narrow, while resonances b, d, and e showed some exchange broadening. At these mixings times all the cross and diagonal peaks were of reasonable intensity.

Table II. Optimized Site-to-Site Rate Constants (s^{-1}) from Magnetization Transfer Data for 1 at 275 K

	rate constants									
constraints applied[a]	k_{ab}	k_{ac}	k_{ad}	k_{ae}	k_{bc}	k_{bd}	k_{be}	k_{cd}	k_{ce}	k_{de}
none	1.26	34.20	−0.40	0.52	−0.06	0.11	0.11	0.74	0.26	0.70
A	1.13	33.72	0.0	0.0	0.0	0.10	0.12	0.55	0.51	0.69
B	1.13	33.72	0.0	0.0	0.0	0.11	0.11	0.54	0.51	0.69
C	1.13	33.72	0.0	0.0	0.0	0.11	0.11	0.53	0.53	0.69
D	1.12	33.67	0.0	0.0	0.0	0.12	0.12	0.54	0.54	0.66
E	1.09	33.64	0.0	0.0	0.0	0.12	0.12	0.54	0.54	0.66
F	1.14	33.54	−0.03	−0.05	−0.01	0.11	0.11	0.57	0.57	0.68
G	1.07	34.23	0.0	0.0	0.0	0.13	0.13	0.0	0.69	0.82
H	1.36	34.16	0.0	0.0	0.0	0.0	0.0	0.57	0.54	0.71

[a] The applied constraints were as follows: A, $k_{ad} = k_{ae} = k_{bc} = 0$; B, as previous plus $k_{bd} = k_{be}$; C, as previous plus $k_{cd} = k_{ce}$; D, as previous plus $k_{bd} + k_{cd} = k_{de}$; E, as previous plus $k_{ba} = k_{cd}$; F, as previous except $k_{ad} \neq k_{ae} \neq k_{bc} \neq 0$; G, see text; H, $k_{ad} = k_{ae} = k_{bc} = k_{bd} = k_{be} = 0$.

chose to examine the multisite exchanges in 1 using the quantitative 1D magnetization transfer method of Grassi et al.[27]

1D Magnetization Transfer Studies. If nonequilibrium magnetization is induced at one site undergoing chemical exchange, then that magnetization will migrate to other sites involved in the exchange. This is the basis of the well-known Forsén–Hoffman[28] method for determining slow-exchange rate constants. In a two-site exchange the rate constant may be obtained without difficulty, and recently Grassi et al.[27] have described a matrix method that allows all exchange rate constants in multisite exchange to be evaluated. This method has the added advantage of allowing constraints to be introduced into the analysis.

In separate experiments, signals b–e were selectively inverted using a DANTE pulse train,[29] and the development of nonequilibrium magnetization followed over a period of 1 s. Experimental intensities were fitted to optimized rate constants and T_1 values, using the procedure described by Grassi et al.[27] Since inversion recovery experiments showed that the T_1 value for all sites was around 1.1 s, only one T_1 value was optimized. Previous work[27] has shown that the derived rate constants are insensitive to T_1 values. Data were analyzed by iteration of all the variables against two, three, and finally all four experimental data sets, and constraints were applied to test hypotheses. The results were closely similar in each case, and the optimized rates obtained from the analysis using all four data sets are set out in Table II.

All rate constants were initially treated as independent variables, and optimization gave $T_1 = 1.10$ s and a least-squares error of 0.0176. All data points were fitted better than the error in integration of ±2 (arbitrary) units. Since the rate constants k_{ad}, k_{ae}, and k_{bc} became negative in all or some of the analyses, these were then set to zero, modestly increasing the least-squares error to 0.0191. Since $k_{bd} \approx k_{be}$ and $k_{cd} \approx k_{ce}$, as indicated by the EXSY data, these were then constrained to be equal, resulting in only a marginal increase in the least-squares error to 0.0195. It was now apparent that $k_{bd} + k_{cd} \approx k_{de}$, suggesting that two independent processes contribute to the d/e exchange. Applying this constraint raised the least-squares error to 0.0204, but all data points were still fitted better than experimental error. Finally, since k_{ba} (i.e. $k_{ab}/2$) was approximately equal to k_{cd}, they were so constrained, giving a least-squares error of 0.0206 for the fully constrained set E (Table II). Reassuringly, releasing the constraint $k_{ad} = k_{ae} = k_{bc} = 0$ at this point resulted in near-zero values for these rates and a lowering of the least-squares error to 0.0197. The value of T_1 remained 1.10 s throughout, which was identical to a crude measurement from inversion recovery experiments. Representative plots of the calculated and experimental magnetizations at each site after inversion of resonance e are shown in Figure 4.

Scheme I

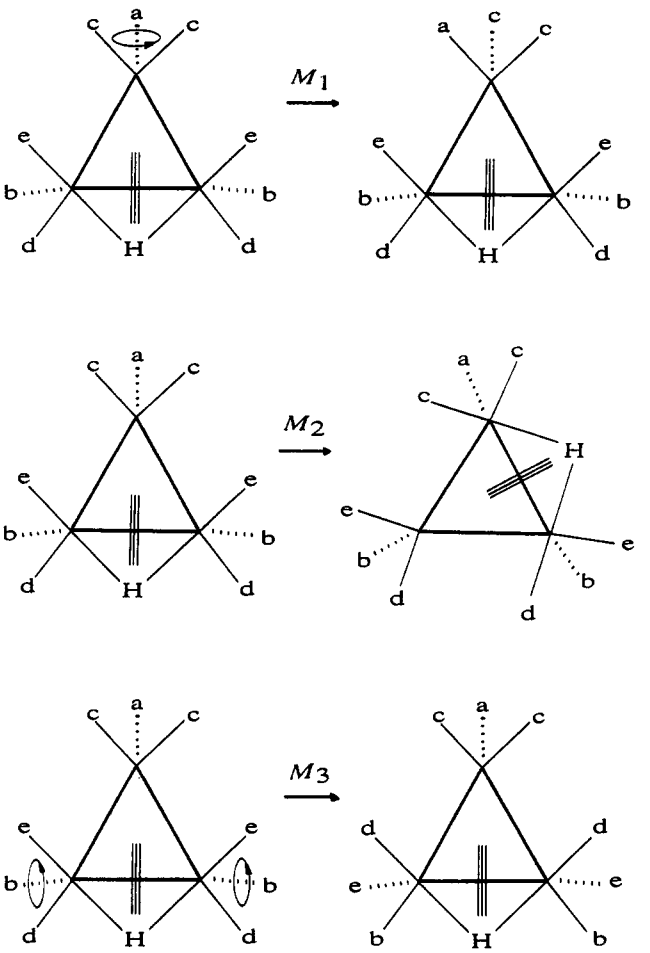

The data are consistent with three fluxional (degenerate permutational) modes M_1–M_3, shown in Scheme I, and having mechanistic rate constants K_1–K_3. Mode M_1 is the tripodal rotation of the unique $Ru(CO)_3$ group which exchanges a and c. Mode M_2 is the rotation of the alkynyl ligand in concert with hydride migration, which results in the exchange of a and b and the cyclical exchange of c, d, and e. It requires that $(k_{ab}/2) = k_{ba} = k_{cd} = k_{ce} = k_{de}$. The final mode M_3 is the tripodal rotation of the two equivalent $Ru(CO)_3$ groups, which requires $k_{bd} = k_{be} = k_{de}$. Since

(27) Grassi, M.; Mann, B. E.; Pickup, B. T.; Spencer, C. M. *J. Magn. Reson.* **1986**, *69*, 92.
(28) (a) Forsén, S.; Hoffman, R. A. *J. Chem. Phys.* **1963**, *39*, 2892. (b) Forsén, S.; Hoffman, R. A. *Acta Chem. Scand.* **1963**, *17*, 1787.
(29) Morris, G. A.; Freeman, R. *J. Magn. Reson.* **1978**, *29*, 433.

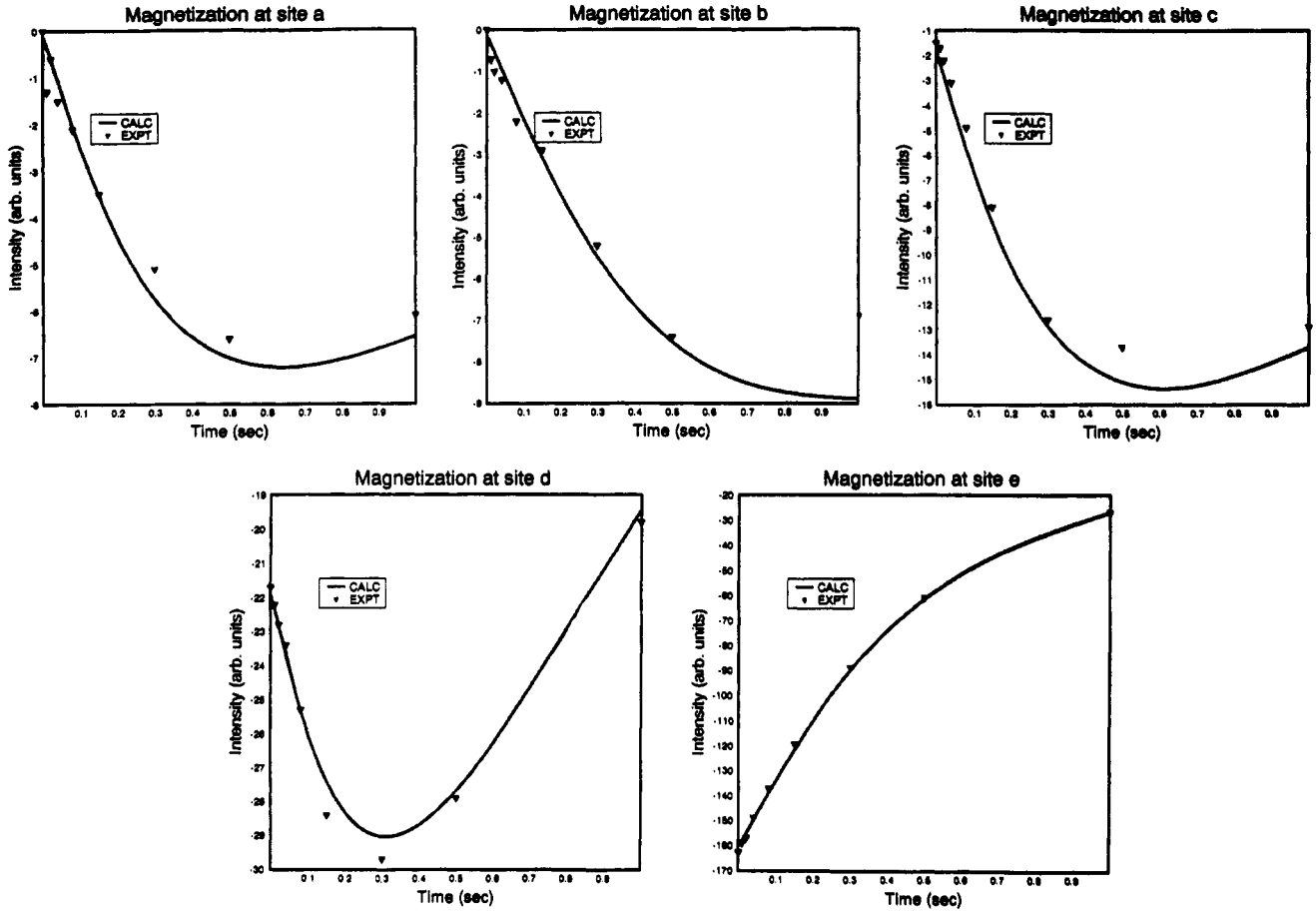

Figure 4. Time dependence of observed and calculated magnetizations at sites a–e, after inversion at site e.

there are two independent modes which exchange d and e, the observed site-to-site rate constant k_{de} is the sum of the rates due to K_2 and K_3. The mechanistic rate constants K are related[23] to the site-to-site rate constants (k_{ij}) by

$$k_{ij} = (\boldsymbol{P}_{ij})K$$

$\boldsymbol{P}_{ij}$ are the elements of the probability matrix $\boldsymbol{P}$ and are merely the probabilities that one passage through the fluxional mode will transfer nucleus i to site j. Consideration of the $\boldsymbol{P}$ matrices for the three fluxional modes leads to the rate constants K_1 = 33.6 (±3.0), K_2 = 1.09 (±0.05), and K_3 = 0.12 (±0.03) s^{-1}. These give $\Delta G^{\ddagger}$ values at 275 K of 59.1 (5), 67.0 (5), and 72.0 (8) kJ mol^{-1}, respectively. We cannot determine whether the mode M_3 occurs as a correlated rotation of both $Ru(CO)_3$ groups (with K_3 = 0.12 s^{-1}) or as uncorrelated motions of each group (with K_3 = 0.24 s^{-1}). Note that the operation of the modes M_1–M_3 will result in complete scrambling of the CO ligands, as is observed, *without* any intermetallic CO migration. Of course, we cannot exclude the possibility that intermetallic exchange processes occur at higher temperatures.

Despite the fact that the large value of K_1 (2 orders of magnitude greater than K_3) dominates the magnetization transfer effects, our data are sufficiently sensitive to the slower rates to exclude specifically several other possibilities. Aime et al.[7,8] have suggested that a merry-go-round exchange occurs in 1. Such an exchange occurring between the equatorial carbonyls c, d, and e would result in the exchanges c ⇔ e ⇔ d but no exchange between c and d. Setting $k_{cd} = k_{ad} = k_{ae} = k_{bc} = 0$, $k_{bd} = k_{be}$, and $k_{bd} + k_{ce} = k_{de}$ (i.e. a merry-go-round exchange in concert with modes M_1 and M_3, constraint set G, Table II) resulted in a large least-squares error of 0.278, with many points fitted considerably worse than experimental error. Since K_3 is small, we also considered the possibility of a zero rate (constraint set H, Table II). This gave a significantly increased least-squares error of 0.071, again with many points fitted worse than experimental error. The fluxional modes M_1–M_3, with associated rate constants K_1–K_3, thus provide the best fit for the data. Finally we note that when these rate constants were used to compute EXSY spectra, the calculated spectral intensities were in agreement with experimental results, within the margins of error. In particular, they correctly predict the intensities of the second-order cross peaks I_{bc} (see Figure 3) and I_{ad} and I_{ae}, which arise from the consecutive operation of modes M_2 followed by M_1.

Our results show that the previous interpretation[8-10,12,20] of the fluxional behavior of 1 is incorrect, and we wish to point out here one particularly important misinterpretation. Rosenberg et al.[20] have reported a kinetic deuterium isotope effect (k_H/k_D = 2) for the single rate constant used by them to simulate the exchange of resonances b, d, and e in 1 and attribute this to either an opening of the hydride bridge or the formation of a μ_3-hydride to allow carbonyl mobility during the "tripodal rotation" of the adjacent $Ru(CO)_3$ groups. This is a surprising result, particularly since the same authors do not observe[20] such an effect in the similar tripodal rotation of the $Os(CO)_3$ groups in $Os_3(\mu\text{-}H)_2(CO)_{10}$. As stated above, it is not possible to simulate adequately the line broadening of resonances b, d, and e by using only one rate constant. Inspection of Figure 4 of ref 20 shows that while the line broadening of resonances d and e is adequately reproduced, the fit to resonance b is poor. Coupled with the reported[8,9] $\Delta G^{\ddagger}$ value of 65.3 (±2) kJ mol^{-1} for this "tripodal exchange", which is identical within error to our value[30] for exchange

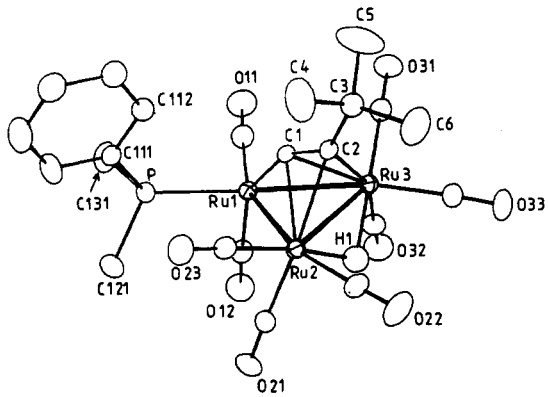

Figure 5. Molecular structure and atomic labeling for **2**. Carbonyl carbon atoms have the same label as attached oxygen atoms.

mode M_2, it is clear that the kinetic deuterium isotope effect reported by Rosenberg et al.[20] refers to M_2, i.e. the rotation of the alkynyl ligand, coupled with a hydride migration. It is entirely reasonable that mode M_2 shows a kinetic deuterium isotope effect, since Ru–H bonds are broken and made during this process. The erroneous conclusion of Rosenberg et al.[20] concerning the kinetic deuterium isotope effect in **1** has also been applied to the interpretation of the fluxionality of other related systems such as $Hg[Ru_3\{\mu_3\text{-}\eta^2\text{-}C{\equiv}C^tBu\}(CO)_9]_2$.[31] In view of our work, these conclusions may also be in error.

It is generally assumed that the exchange of carbonyls within $M(CO)_3$ groups occurs in a concerted fashion, i.e. a tripodal rotation. The results of Hawkes et al.[32] on the σ,π-allyl cluster $Ru_3(\mu\text{-}H)\{\mu_3\text{-}\eta^3\text{-}MeCC(H)CMe\}(CO)_9$, which show experimentally equal rate constants for the exchange of the three chemically inequivalent CO's in an $Ru(CO)_3$ group, are strongly in favor of such a concerted mechanism. It is not clear, however, that this should also be the case in the $M(CO)_2(PR_3)$ group, since this rotation does not have the 3-fold degeneracy of the unsubstituted case.

In an attempt to address this question, Rosenberg et al.[11] have examined the fluxionality of a phosphine derivative of **1**, namely $Ru_3(\mu\text{-}H)(\mu_3\text{-}\eta^2\text{-}C{\equiv}C^tBu)(CO)_8(PMeBzPh)$, which contains the chiral phosphine PMeBzPh. Two mechanisms for CO exchange were considered, (i) concerted rotation of the $Ru(CO)_2(PMeBzPh)$ group, which results in exchange of diastereomers, and (ii) pairwise CO exchange within diastereomers. The mode of collapse of the ^{13}C carbonyl signals, arising from the $Ru(CO)_2$-(PMeBzPh) groups of the two NMR-distinguishable diastereomers, supports the concerted mechanism. However, this experiment suffers from some potential drawbacks, particularly since the expected exchange-averaged chemical shifts do not differ markedly between the two mechanisms considered. No rates measurements were reported, and the variation with temperature both of chemical shifts (which can be quite marked) and the diastereomer populations could only be estimated, casting some doubt on the conclusion.

A more straightforward method to determine whether the exchange in an $M(CO)_2(PR_3)$ group occurs in a concerted fashion is to use a prochiral phosphine, since this can provide an independent measurement of the rate of enantiomerization. For this reason we have prepared, and examined the fluxional behavior of $Ru_3(\mu\text{-}H)(\mu_3\text{-}\eta^2\text{-}C{\equiv}C^tBu)(CO)_8(PMe_2Ph)$ (**2**).

Table III. Final Positional Parameters (Fractional Coordinates) with Esd's in Parentheses and Isotropic Thermal Parameters (Å²; Equivalent Isotropic Parameters U_{eq} for Anisotropic Atoms) for $Ru_3(\mu\text{-}H)(\mu_3\text{-}\eta^2\text{-}C{\equiv}C^tBu)(CO)_8(PMe_2Ph)$ (2)[a]

atom	x/a	y/b	z/c	U_{eq}
Ru(1)	0.87279 (3)	0.18411 (1)	0.37080 (2)	0.040
Ru(2)	0.61851 (3)	0.14604 (1)	0.29903 (2)	0.041
Ru(3)	0.82056 (3)	0.16571 (1)	0.15135 (2)	0.042
P	0.86291 (11)	0.16615 (5)	0.55413 (7)	0.049
O(11)	1.1690 (3)	0.1921 (2)	0.3641 (3)	0.094
O(12)	0.8410 (5)	0.3240 (2)	0.4012 (3)	0.102
O(21)	0.5227 (4)	0.2674 (2)	0.3993 (3)	0.092
O(22)	0.3880 (3)	0.1201 (2)	0.1468 (3)	0.100
O(23)	0.5155 (3)	0.0736 (2)	0.4916 (3)	0.080
O(31)	1.0960 (3)	0.1247 (2)	0.0878 (3)	0.090
O(32)	0.8843 (4)	0.3039 (2)	0.1292 (3)	0.093
O(33)	0.6942 (5)	0.1519 (2)	−0.0703 (3)	0.109
C(1)	0.8206 (3)	0.1069 (2)	0.2977 (3)	0.038
C(2)	0.7549 (3)	0.0748 (2)	0.2261 (3)	0.042
C(3)	0.7392 (4)	0.0085 (2)	0.1851 (3)	0.057
C(4)	0.6839 (10)	−0.0313 (3)	0.2745 (5)	0.131
C(5)	0.8715 (7)	−0.0165 (3)	0.1588 (8)	0.146
C(6)	0.6518 (8)	0.0034 (3)	0.0898 (5)	0.119
C(11)	1.0560 (5)	0.1894 (2)	0.3691 (3)	0.061
C(12)	0.8544 (5)	0.2713 (2)	0.3915 (3)	0.065
C(21)	0.5624 (5)	0.2226 (2)	0.3629 (3)	0.064
C(22)	0.4702 (4)	0.1271 (2)	0.2069 (3)	0.062
C(23)	0.5561 (4)	0.0994 (2)	0.4196 (3)	0.055
C(31)	0.9933 (5)	0.1403 (2)	0.1118 (3)	0.061
C(32)	0.8618 (4)	0.2529 (2)	0.1401 (3)	0.064
C(33)	0.7416 (5)	0.1548 (2)	0.0114 (3)	0.067
C(111)	0.8265 (4)	0.0874 (2)	0.6004 (3)	0.049
C(112)	0.8471 (5)	0.0368 (2)	0.5368 (3)	0.059
C(113)	0.8262 (6)	−0.0233 (2)	0.5748 (4)	0.073
C(114)	0.7859 (5)	−0.0321 (3)	0.6758 (4)	0.078
C(115)	0.7636 (8)	0.0161 (3)	0.7397 (4)	0.103
C(116)	0.7829 (7)	0.0768 (3)	0.7028 (4)	0.095
C(121)	0.7456 (6)	0.2143 (2)	0.6256 (4)	0.085
C(131)	1.0160 (6)	0.1817 (3)	0.6259 (4)	0.085
H(1)	0.655 (5)	0.191 (2)	0.192 (4)	0.080

[a] $U_{eq} = {}^1/_3\sum_i\sum_j U_{ij}a_i^*a_j^*\mathbf{a}_i\cdot\mathbf{a}_j$.

Table IV. Selected Bond Lengths (Å) and Bond Angles (deg) for 2

Ru(1)–Ru(2)	2.8384 (4)	Ru(1)–Ru(3)	2.8045 (4)
Ru(2)–Ru(3)	2.7924 (4)	Ru(1)–P	2.3158 (9)
Ru(1)–C(1)	1.959 (3)	Ru(2)–C(1)	2.212 (3)
Ru(3)–C(1)	2.214 (3)	Ru(2)–C(2)	2.254 (3)
Ru(3)–C(2)	2.261 (3)	Ru(1)–C(11)	1.859 (5)
Ru(1)–C(12)	1.897 (4)	Ru(2)–C(21)	1.911 (5)
Ru(2)–C(22)	1.925 (4)	Ru(2)–C(23)	1.914 (4)
Ru(3)–C(31)	1.901 (5)	Ru(3)–C(32)	1.921 (5)
Ru(3)–C(33)	1.924 (4)	Ru(2)–H(1)	1.69 (5)
Ru(3)–H(1)	1.84 (5)	C(1)–C(2)	1.304 (5)
mean C–O(carbonyl)		1.133 (6)	
Ru(2)–Ru(1)–P	102.5 (1)	Ru(3)–Ru(1)–P	157.8 (1)
Ru(1)–C(1)–C(2)	153.8 (3)	C(1)–C(2)–C(3)	140.8 (4)
Ru(2)–H(1)–Ru(3)	104 (2)		

Fluxional Behavior of 2. The derivative **2**, which does not appear to have been previously reported, was made by a standard method (see Experimental Section). Although the NMR data showed that the major isomer in solution was identical to previously reported monophosphine derivatives of **1**, the presence of isomers in solution prompted a determination of the solid-state structure of **2**. Figure 5 shows the molecular structure and atomic labeling scheme, while Tables III and IV give the positional parameters and important metrical parameters. The phosphine substitutes in an equatorial site in the unique Ru-

(30) Using our value of $\Delta G^{\ddagger}$ of 67.0 kJ mol^{-1}, we estimate a rate constant of 12 s^{-1} at 299 K for mode M_2. This compares very favorably with the rate constant of 15 s^{-1} determined by Rosenberg et al.[20] for the "tripodal rotation" of the $Ru(CO)_3$ groups.

(31) Hajela, S.; Novak, B. M.; Rosenberg, E. *Organometallics* **1989**, *8*, 468.

(32) Hawkes, G. E.; Lian, L. Y.; Randall, E. W.; Sales, K. D. *J. Magn. Reson.* **1985**, *65*, 173.

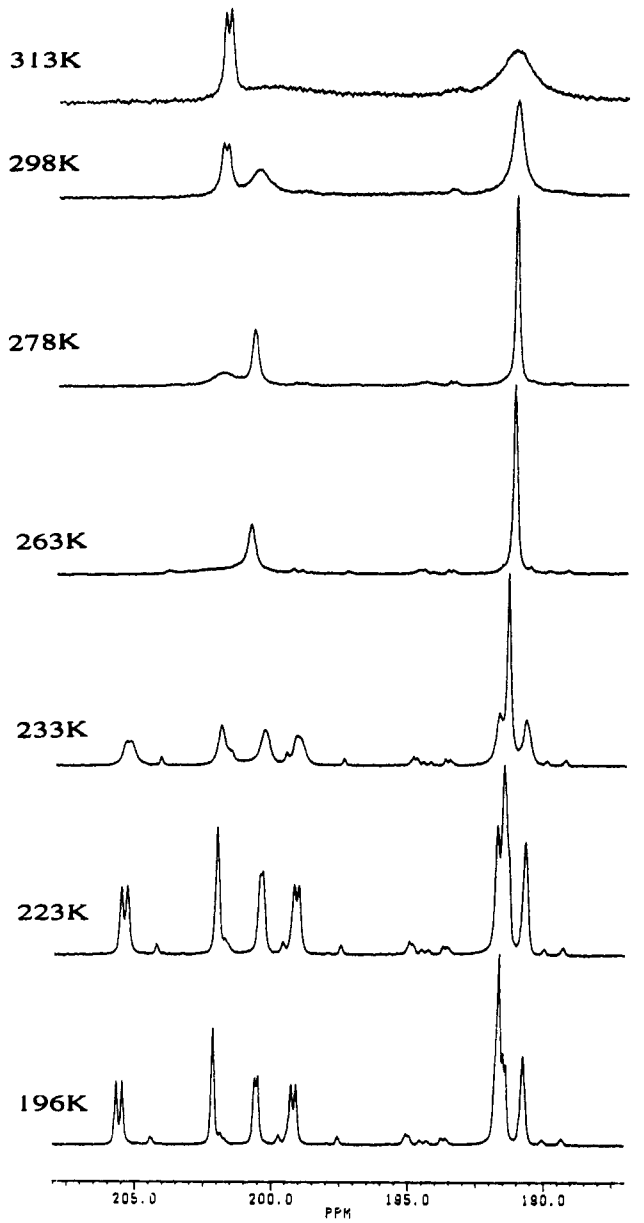

Figure 6. Variable-temperature $^{13}C\{^1H\}$ NMR spectra of **2** in the carbonyl region.

$(CO)_3$ group, giving a structure identical to that reported[33] for $Ru_3(\mu\text{-}H)(\mu_3\text{-}\eta^2\text{-}C{\equiv}C^tBu)(CO)_8(PPh_2OEt)$ (**3**). The Ru(1)–Ru(2) and Ru(1)–Ru(3) distances of 2.8384 (4) and 2.8045 (4) Å, respectively, are longer than found in **1** (average distance 2.797 Å[18]), while the Ru(2)–Ru(3) distance of 2.7924 (4) Å is identical to that found in **1**. The phosphine thus elongates the non-hydride-bridged vectors, with the longest one being cis to the phosphine, presumably due to steric congestion between the ^{t}Bu group and the phosphine. There is little difference in the Ru–$C_{alkynyl}$ separations in **1** and **2**, suggesting that the primary effect of phosphine substitution is in the metal skeleton. Very similar observations were made for **3**.[33]

^1H, ^{13}C, and ^{31}P NMR spectra of **2** show evidence for three isomers[34] of **2** in solution. In addition to signals from the main isomer **2a** given in Table V, there are weak resonances at low temperatures due to **2b** (ca. 10%) [$\delta(^1H)$ −20.28 (J_{PH} = 8.7 Hz); $\delta(^{31}P)$ 5.3] and **2c** (ca. 7%) [$\delta(^1H)$ −20.42 (J_{PH} = 7.5 Hz); $\delta(^{31}P)$ −2.4]. Resonances due to **2b** and **2c** broaden considerably on raising the temperature, and at 298 K the two hydride signals collapse to a broad doublet, suggesting that **2b** and **2c** exchange with each other. On further increase of the temperature to 377 K, only a single broad hydride resonance is observed, indicating complete exchange between **2b**/**2c** and **2a**, and from band shape analysis we estimate a $\Delta G^{\ddagger}$ value of 70.5 (±1.0) kJ mol^{-1} for this process. Isomers **2b** and **2c** are assigned to the species with the phosphine in an axial or equatorial site cis to the hydride ligand (i.e. replacing the CO ligands CO(21) or CO(22), respectively; see Figure 5). The exchange between **2b** and **2c** is accomplished by a tripodal rotation of the $Ru(CO)_2(PMe_2Ph)$ group, while the exchange between **2b**/**2c** and **2a** occurs through rotation of the alkynyl ligand, similar to M_2 in **1**. We note that isomers have not been previously reported for the other monophosphine derivatives of **1**.[9,11]

Table V. NMR Parameters for 2a

reson	chem shift/ppm	mult[a]	J/Hz P	J/Hz H
	^{13}C Data[b]			
a	205.7	d	11.4	
b	202.4	s		<3
c	200.6	d	5.9	<3
d	199.3	d	9.0	
e[c]	191.9	s		12.4
f[c]	191.7	s		<3
g	191.6	d	5.6	<3
h	190.8	s		13.2
C_α	163.7	s		
C_β	112.6	s		
	^{31}P Data[d]			
	18.7	s		
	^1H Data[e]			
Ru(μ-H)Ru	−21.11	d	1.8	
Me(^{t}Bu)	1.41	s		
Me	2.02	d	9.2	
Ph	8.0–7.6	m		

[a] Multiplicities for ^{13}C refer to ^1H-decoupled spectra. [b] CD_2Cl_2, 196 K. [c] These signals are isochronous at 196 K; shifts given at 223 K. [d] CD_2Cl_2, 263 K. [e] CD_2Cl_2, 298 K.

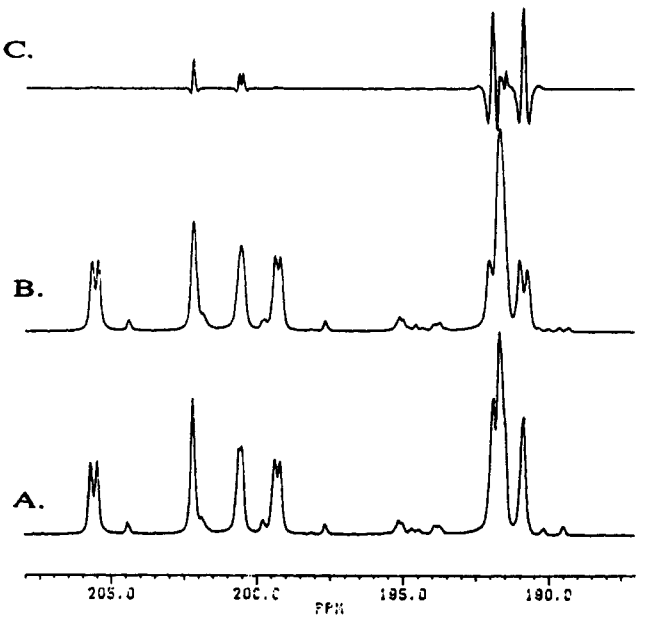

Figure 7. Decoupling difference ^{13}C spectra of **2** at 223 K: (A) ^1H-decoupled spectrum; (B) ^1H-coupled spectrum; (C) spectrum A − spectrum B.

(33) Carty, A. J.; MacLaughlin, S. A.; Taylor, N. J.; Sappa, E. *Inorg. Chem.* **1981**, *20*, 4437.

(34) The weak signals are definitely not due to impurities, since a large, flawless single crystal of **2**, when dissolved in CD_2Cl_2, showed signals exactly similar (in the same intensity ratio) to a bulk sample.

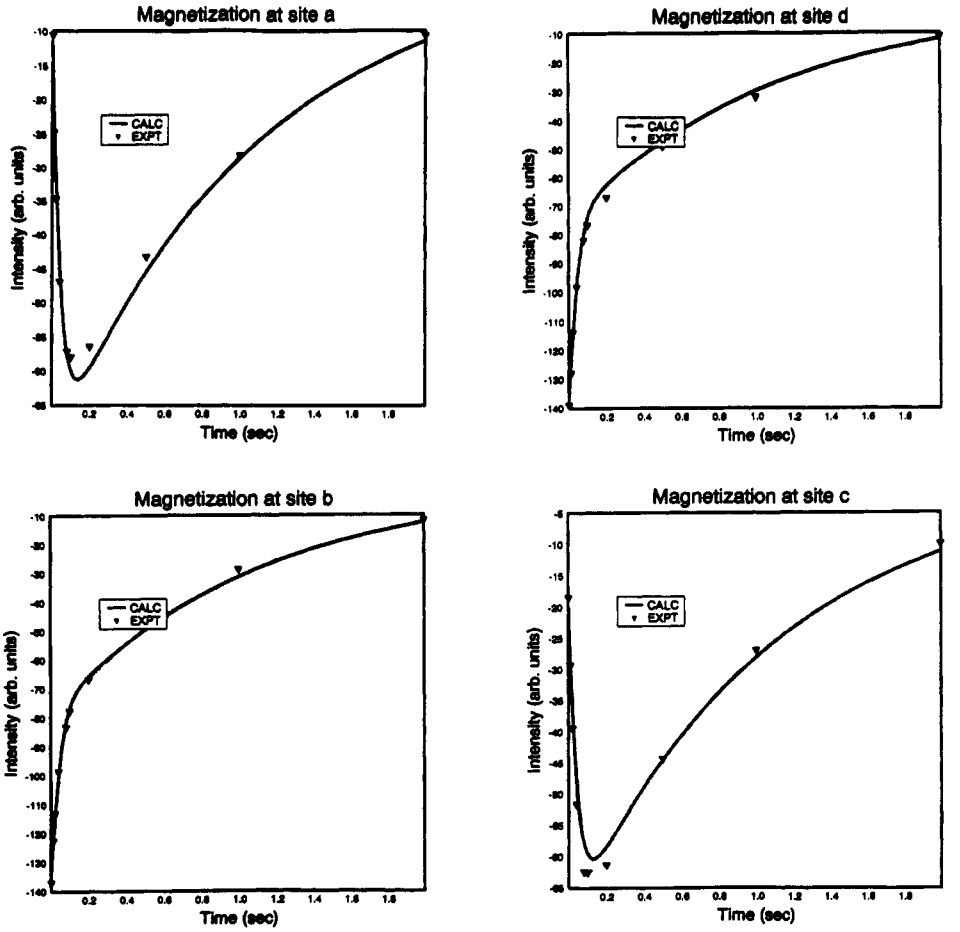

Figure 8. Time dependence of observed and calculated magnetizations: (top) magnetizations at sites a and d after inversion at site d; (bottom) magnetizations at sites b and c after inversion at site b.

The variable-temperature ^{13}C NMR spectra of **2** are shown in Figure 6 and are quite similar to those reported by Jangala et al.[9] for the PPh_3 analogue. Three resonances at $\sim\delta$ 193 are poorly resolved at low temperatures, though assignments are greatly aided by the ^1H decoupling difference spectrum shown in Figure 7. Since resonances a and d show no coupling to the hydride and have the largest ^{31}P coupling, they are assigned to the carbonyls in the $Ru(CO)_2(PMe_2Ph)$ group, while resonances e and h show a large trans coupling to the hydride. Resonances b, c, f, and g show smaller cis couplings to the hydride. An EXSY spectrum at 223 K (t_m = 0.2 s) shows that resonance a exchanges with d, resonance b with c, and resonance e with h. The expected exchange of f and g cannot be observed, since they are isochronous. The assignments shown in Chart II are tentative and are based on chemical shift arguments. Since a resonates some 6 ppm to high frequency of d, it is assigned to the axial CO. The pairs b/c and e/h are assigned on the basis of their $\Delta\delta$ as compared with **1**, since it may be expected that the carbonyls close to the phosphine are shifted more relative to **1** than those further away. It should be stressed that the relative assignments of the exchanging pairs in no way affects the arguments about the fluxional behavior, which are detailed below.

The temperature dependence of the ^{13}C spectrum between 196 and 313 K is readily interpretable in terms of two basic fluxional processes. The lowest energy process exchanges a and d and also results in a time-averaged molecular mirror plane (i.e. cluster enantiomerization), apparently at the same or a similar rate. At 278 K resonances b and c have coalesced to a broad singlet at δ 201.7, while a and d coalesce to a doublet (J_{PC} = 9.5 Hz) at their mean chemical shift of δ 202.7 at slightly higher temperatures. The remaining four carbonyls give an averaged resonance at δ 192.1, which is at the mean of the e/h and f/g pairs. Above 278 K a second process, presumably a tripodal rotation of the $Ru(CO)_3$ groups, begins to average all carbonyls except a and d. Above 350 K the onset of total CO scrambling occurs, presumably through bridged intermediates.

It is the low-energy process which interests us, since it involves cluster enantiomerization. Regarding the $Ru(CO)_2(PMe_2Ph)$ group, there are four permutomers relevant to this exchange, shown in Scheme II. There are six permutationally distinct exchange modes, M_1–M_6, between these permutomers, although only three modes, M_1–M_3 (proceeding at rates K_1–K_3), are NMR distinguishable. Exchange M_1 corresponds to a tripodal rotation, which exchanges a and d and results in cluster enantiomerization. Exchange M_2 is the pairwise exchange of a and d without cluster enantiomerization, while exchange M_3 involves pairwise exchange between the phosphine and carbonyl d and, hence, results in cluster enantiomerization without a/d exchange. The experimentally measurable rate constant k_{ad} is thus $K_1 + K_2$, while the rate of enantiomerization is given by $K_1 + K_3$.

In the absence of unlikely processes involving pairwise exchange between the axial carbonyls b and c, the rate of enantiomerization may be measured by k_{bc}. Kinetic analysis of the EXSY spectrum at 223 K gave values of 6.9 (±1.5) s^{-1} for k_{ad} and 9.1 (±1.5) s^{-1} for k_{bc}. Although these are equal within error, we also carried out 1D magnetization transfer experiments at the same temper-

Chart II

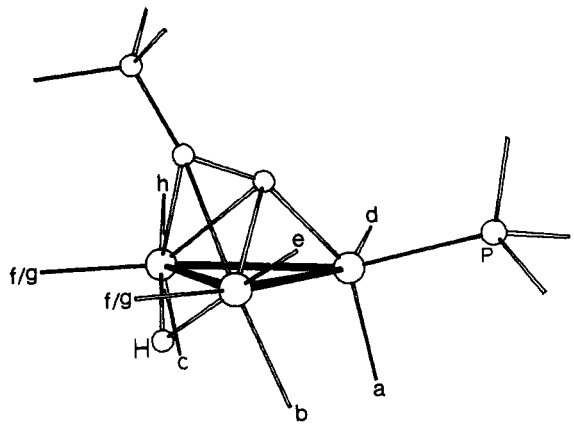

Scheme II

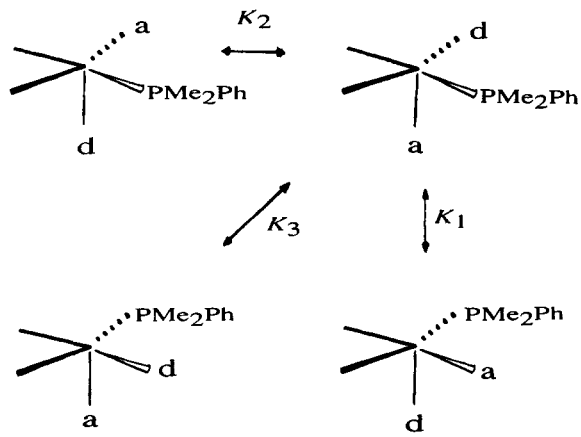

ature to convince ourselves further. Selective inversion of resonances a to d by a DANTE pulse train, followed by observation of the magnetization at these sites over a 2-s period (Figure 8), afforded values of 10.8 s^{-1} for k_{ad} and 11.6 s^{-1} for k_{bc}, with T_1 = 1.08 s and a least-squares error of 0.088. Constraining k_{ad} to equal k_{bc} resulted in a rate constant of 11.2 s^{-1} and an insignificant rise in the least-squares error to 0.089. This confirms that the two rate constants are identical within experimental error. The accuracies of integrations are worse than for **1**, because of overlapping signals from the minor isomers **2b** and **2c**. Since these minor signals remain sharp up to 250 K, they are not involved in exchange with **2a** at 223 K and do not affect the derived rate constants.

As a further check on the rate of enantiomerization, we measured the rate of exchange between the diastereotopic methyl groups of the phosphine in the ^{13}C spectrum by band shape analysis (Figure 9). This analysis gave $\Delta H^{\ddagger}$ = 57.3 (±1.3) kJ mol^{-1} and $\Delta S^{\ddagger}$ = 35.1 (±5.6) J mol^{-1} K^{-1}, with a $\Delta G^{\ddagger}$ value at 240 K of 48.8 (±0.4) kJ mol^{-1}.[35] Hence at 223 K, the rate constants for enantiomerization (11.8 s^{-1}) and k_{bc} are identical, consistent with our assumption. It follows that $K_1 + K_3 = K_1 + K_2$, and since it is highly unlikely that K_2 and K_3 are equal and nonzero, this implies that a single process M_1, i.e. concerted tripodal rotation of the $Ru(CO)_2(PMe_2Ph)$ group, is responsible for the low-energy exchanges observed for **2a**.

Conclusions

The tripodal rotation of the $Ru(CO)_2(PMe_2Ph)$ group in **2a** has an activation barrier some 10 kJ mol^{-1} lower than for the $Ru(CO)_3$ rotation in **1**, suggesting that steric factors are unimportant in this process. We have previously[36] noted similar results for phosphine derivatives of $Os_3(\mu\text{-}H)_2(CO)_{10}$. The small positive entropy of activation is consistent with intramolecular exchange.

Our investigations have also shown that, for **1**, the next highest energy process is a degenerate process involving rotation of the alkynyl ligand coupled with concerted motion of the hydride. Such a process also accounts for the exchange between isomers **2a** and **2b**/**2c**. The barriers to the alkynyl rotation in **1** and **2** parallel those for similar processes examined by Predieri et al.[14a] (57.8 kJ mol^{-1}), and Chi et al.[15] (61–72 kJ mol^{-1}). Interestingly, for the $Ph_2PCH_2CH_2EPh_2$ (E = P, As) derivatives of **1**, there is no evidence for alkynyl rotation.[14b]

Table VI. Experimental Data for the Crystallographic Study

compd formula	$C_{22}H_{21}O_8PRu_3$
M_r	747.59
space group	$P2_1/n$
cryst system	monoclinic
a/Å	10.1257 (7)
b/Å	21.432 (2)
c/Å	12.440 (1)
β/deg	90.448 (6)
Z	4
V/Å^3	2699.6 (4)
D_{calc}/g cm^{-3}	1.839
$F(000)$	1456
μ(Mo Kα)/cm^{-1}	17.25
θ range/deg	$2 < \theta < 25$
cryst size/mm	0.8 × 0.7 × 0.4
range of trans coeff corr	1.23/0.81
no. of data collcd	5159
no. of unique data	4724
hkl range	0–12, 0–25, −14 to +14
R_{merge}	0.039 (before abs corr) 0.032 (after abs corr)
std reflcns	2,15,0; 6,10,$\bar{1}$; $\bar{5}9\bar{5}$
observability criterion n ($I > n\sigma(I)$)	3.0
no. of data in refinement	4189
no. of refined params	310
final R	0.028
final R_w	0.039
largest remaining feature in electron dens map/e Å^{-3}	+0.43, −0.61
shift/esd in last cycle	0.014 (max) 0.002 (mean)

Experimental Section

General experimental methods were as previously detailed.[17] NMR spectra were measured on a Bruker AM200SY instrument equipped with an array processor and process controller. ^1H (200.13 MHz) and ^{13}C (50.32 MHz) spectra were referenced to internal solvent signals and are reported relative to $SiMe_4$. ^{31}P (81.02 MHz) spectra are referenced to 85% H_3PO_4. All ^{13}C NMR measurements were made on ^{13}CO-enriched samples (ca. 40% ^{13}C). NMR probe temperatures were calibrated by using the method of van Geet[37] and are considered accurate to ±2 K. Band shape analysis was carried out by using a locally adapted version of DNMR3.[38] EXSY spectra were recorded in pure absorption mode by using the Bruker microprogram NOESYPH. The data table was acquired by using 1024 words in the f_2 dimension and 256 words in the f_1 dimension, zero filled to 1 K. Spectral widths were typically 1 kHz, and recycle delays 4–6 s. Eight scans per f_1 increment were used, and a random variation of ±15% was applied to the mixing time delay to reduce any correlations arising from scalar coupling. Spectra were processed with minimal line broadening (typically 2–5 Hz) in f_2 and the necessary line broadening in f_1 to alleviate truncation errors (typically 5–10 Hz).

(35) This is essentially identical to the value for $\Delta G^{\ddagger}$ of 49.7 (±2) kJ mol^{-1} quoted[9] for the same process in the PPh_3 analogue of **2**.

(36) Farrugia, L. J. *J. Organomet. Chem.* **1990**, *394*, 515.
(37) van Geet, A. L. *Anal. Chem.* **1970**, *42*, 679.
(38) Kleier, D. A.; Binsch, G. *QCPE* **1970**, *11*, 165.

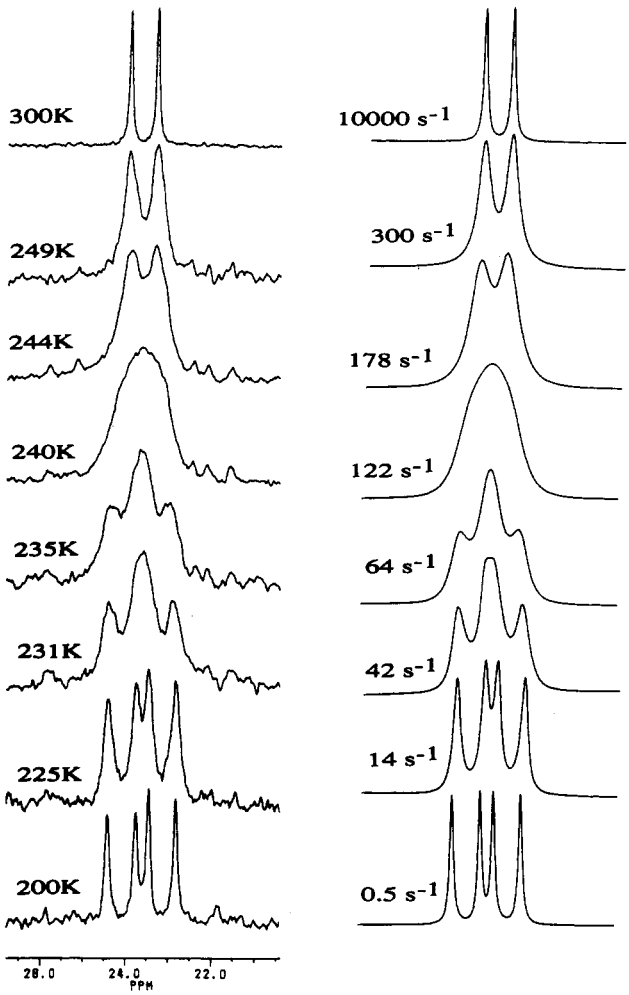

Figure 9. Observed and simulated variable-temperature $^{13}C\{^1H\}$ spectra of **2** in the phosphine methyl region.

2D integrals were measured by using the box-integral routine of the Bruker AP2D display program. Errors in the integrals were estimated from the integrated intensity of identical sized boxes in noise areas of the spectrum. Site-to-site exchange rate constants were obtained from the intensity matrix by using the program D2DNMR.[24]

Magnetization transfer data were acquired by using the methodology outlined by Beringhelli et al.[39] The DANTE 180° selective pulse typically used 30 on-resonance pulses separated by a delay of 1 ms and was calibrated for maximum inversion. For broader signals 20 pulses with a longer pulse width were necessary to achieve good inversion. Eight scans per exchange delay were collected, and the delay was then reset. The whole experiment was cycled 10 times to minimize the effects of temperature and spectrometer drift. The final exchange delay of ca. $5T_1$ was used as a control, and nonequilibrium magnetizations were then obtained by subtracting each spectrum from this one. Line broadening of 10 Hz was used in processing to ensure reasonable signal to noise, and the intensity at each site was obtained by integration. The data were analyzed by using a program described by Grassi et al.[27]

The $^{13}C\{^1H\}$ NOE experiment involved irradiation at the ^{t}Bu ^1H frequency for 10 s, followed by acquisition of a ^1H-coupled spectrum, with an off-resonance acquisition used as a control. Initial studies on cluster **1** were made using a pure sample made up under nitrogen atmosphere in deoxygenated $CDCl_3$. This sample was used for the NOE experiment and some EXSY measurements using a recycle delay of 5 s. Subsequent inversion recovery measurements showed a T_1 of ca. 9 s for the carbonyl ^{13}C signals, so $Cr(acac)_3$ was added to reduce this to ~1 s. Surprisingly, the short recycle delay compared with T_1 did not adversely affect the intensities in the EXSY spectra. It was not necessary to add $Cr(acac)_3$ to the sample of **2**, since the measured T_1 value at 223 K of the pure sample was ~1 s.

Cluster **1** was prepared as previously described[40] and enriched by heating a toluene solution to ca. 100 °C under 1 atm of ^{13}CO (99% ^{13}C) for 3 days. A ^{13}CO-enriched sample of **2** was prepared as described below from a previously enriched sample of **1**.

Preparation of $Ru_3(\mu\text{-}H)(\mu_3\text{-}\eta^2\text{-}C{\equiv}C^tBu)(CO)_8(PMe_2Ph)$ (2). To a stirred solution of $Ru_3(\mu\text{-}H)(\mu_3\text{-}\eta^2\text{-}C{\equiv}C^tBu)(CO)_9$ (0.2 g, 0.31 mmol) in 10:1 CH_2Cl_2/CH_3CN (20 mL) at 0 °C was added an equimolar solution of Me_3NO in CH_2Cl_2 (5 mL). After being stirred for 5 min, a solution of PMe_2Ph (0.31 mmol) in hexane was added, and the solution became a darker orange. After further stirring for 5 min, the volatiles were removed under vacuum and the residues chromatographed on Florosil using hexane/dichloromethane mixtures as an eluant. A first pale yellow band afforded unreacted **1** (0.01 g), and a second bright yellow band afforded the required product. Recrystallization from hexane gave bright yellow crystals of **2** (0.14 g, 61%). Further red/orange and purple bands were not characterized. Characterization data for **2** (see also Table V): IR (C_6H_{12}) ν(CO) 2076 (m), 2052 (vs), 2039 (w), 2023 (w), 2012 (vs), 2003 (s), 1991 (w), 1984 (m), 1966 (vw), 1958 (vw), 1946 (m) cm^{-1}; $^{13}C\{^1H\}$ NMR (CD_2Cl_2, 223 K) δ 136.2 (d, 1 C, J(PC) = 45.1 Hz, Ph), 130.8 (d, 2 C, J(PC) = 13.2 Hz, Ph), 130.5 (s, 1 C, Ph), 128.1 (d, 2 C, J(PC) = 10.5 Hz, Ph), 35.5 (s, 1 C, CMe_3), 34.2 (s, 3 C, $C(CH_3)_3$). Anal. Calcd for $C_{22}H_{21}O_8PRu_3$: C, 35.34; H, 2.83. Found: C, 35.22; H, 2.71.

Crystal Structure Determination. Details of data collection procedures and structure refinement are given in Table VI. A bright yellow crystal of **2** was mounted in a general position on a glass fiber and coated with acrylic resin. Data were collected at ambient temperatures, using the $\theta/2\theta$ scan mode, on a CAD4F automated diffractometer with graphite-monochromated X-radiation (λ = 0.71069 Å). Unit cell parameters were determined by refinement of the setting angles ($14 < \theta < 16°$) of 25 reflections, using the SET4 routine, which averages angles from four diffracting positions. The intensities of three reflections were monitored every 2 h; a decay in intensities of ca. 1% over 44.4 h of data collection was noted and a linear correction applied. *Lp* and absorption/extinction (DIFABS[41]) corrections were also applied. The systematic absences uniquely indicated the centrosymmetric space group $P2_1/n$. The structure was solved by direct methods (MITHRIL[42]) and subsequent electron density difference syntheses. Refinement was by full-matrix least-squares minimizing the function $\sum w(|F_o| - |F_c|)^2$ with the weighting scheme $w = [\sigma^2(F_o)]^{-1}$ used and judged satisfactory. $\sigma(F_o)$ was estimated from counting statistics. All non-H atoms were allowed anisotropic thermal motion. The phenyl and methyl hydrogen atoms were included at calculated positions (C–H = 1.0Å), while the position of the hydride H(1) was determined from a difference Fourier map. Fixed isotropic thermal parameters (0.08 Å^2) were used for all H atoms. Phenyl and methyl hydrogen atoms were allowed to ride on their respective attached C atoms, while positional parameters for H(1) were freely refined. The esd of an observation of unit weight (S) was 2.1. Neutral-atom scattering factors were taken from ref 43 with corrections applied for anomalous scattering. All calculations were carried out on a MicroVAX 3600 computer using the Glasgow GX suite of programs.[44]

Acknowledgment. Dr. B. E. Mann is thanked for helpful advice, and Dr. B. T. Pickup for supplying the program to analyze the magnetization transfer data. Johnson Matthey is thanked for a generous loan of Ru

(39) Beringhelli, T.; D'Alphonso, G.; Molinari, H.; Mann, B. E.; Pickup, B. T.; Spencer, C. M. *J. Chem. Soc., Chem. Commun.* **1986**, 796.

(40) (a) Sappa, E.; Gambino, O.; Milone, L.; Cetini, G. *J. Organomet. Chem.* **1972**, *39*, 169. (b) Rosenberg, E.; Novak, B. *Inorg. Synth.* **1989**, *26*, 329–330. (c) Aime, S.; Milone, L.; Osella, D. *Organomet. Synth.* **1988**, *4*, 256–257.

(41) Walker, N.; Stuart, D. *Acta Crystallogr., Sect. A: Found. Crystallogr.* **1983**, *A39*, 158.

(42) Gilmore, C. J. *J. Appl. Crystallogr.* **1984**, *17*, 42.

(43) *International Tables for X-Ray Crystallography*; Kynoch: Birmingham, England, 1974; Vol. 4.

(44) Mallinson, P.; Muir, K. W. *J. Appl. Crystallogr.* **1985**, *18*, 51.

salts.

Registry No. 1, 57673-31-1; **2a**, 137364-15-9; **2b**, 137364-16-0; **2c**, 137490-29-0.

Supplementary Material Available: Tables of anisotropic thermal parameters, calculated hydrogen positional parameters, and complete bond lengths and bond angles and torsion angles (10 pages); a listing of calculated and observed structure factors (14 pages). Ordering information is given on any current masthead page.

Synthesis and Spectroscopic Investigations of Alkylaluminum Alkoxides Derived from Optically Active Alcohols. The First Structural Identification of an Optically Active Organoaluminum Alkoxide

Michael L. Sierra, Rajesh Kumar, V. Srini J. de Mel, and John P. Oliver*

Department of Chemistry, Wayne State University, Detroit, Michigan 48202

Received February 19, 1991

The reaction of trialkylaluminum, R_3Al (R = Me, Et, *i*-Bu), with optically active alcohols such as *l*-menthol and *l*-borneol in a 1:1 ratio gives high yields of R_2AlOR^* (OR^* = *l*-mentholate, R = Me (**1a**), Et (**1b**), *i*-Bu (**1c**); OR^* = *l*-borneolate, R = Me (**2a**), Et (**2b**), *i*-Bu (**2c**)) and the corresponding alkane, RH. The resulting alkoxides have been characterized by ^1H and ^{13}C NMR spectroscopy. The single-crystal X-ray structures of **1a,c** and **2a** established the dimeric structure for these compounds. **1a** was assigned to the orthorhombic cell system, space group $P2_12_12_1$ (No. 19), with cell constants a = 10.097 (1) Å, b = 10.485 (1) Å, c = 26.920 (4) Å, and Z = 4 (dimers). The structure was refined to a final R = 4.5% (R_w = 3.9%) based on 2669 observed reflections ($F_o \geq 2.5\sigma(F)$). **1c** was assigned to the triclinic cell system, space group $P\bar{1}$ (No. 1), with cell constants a = 10.838 (4) Å, b = 12.792 (6) Å, c = 15.787 (7) Å, α = 81.56 (4)°, β = 83.04 (4)°, γ = 73.01 (3)°, and Z = 2 (dimers). The structure was refined to a final R = 8.7% (R_w = 8.5%) based on 4213 observed reflections ($F_o \geq 3\sigma(F)$). **2a** was assigned to the monoclinic cell system, space group $P2_1$ (No. 4), with cell constants a = 7.261 (7) Å, b = 14.494 (8) Å, c = 12.938 (7) Å, β = 93.63 (7)°, and Z = 2 (dimers). The structure was refined to a final R = 5.3% (R_w = 4.4%) based on 1432 observed reflections ($F_o \geq 2.5\sigma(F)$). In **1a,c** and **2a**, the alkoxide ligands serve as bridging units between the two dialkylaluminum moieties to give stable, planar Al_2O_2 rings. The behavior of the ^1H NMR spectra of **1a–c** as a function of temperature has been interpreted in terms of increasing steric interaction of the *l*-mentholate group with the methyl, ethyl, and isobutyl groups attached to the aluminum. This steric interaction gives rise to restricted rotation of the *l*-mentholate and/or the alkyl group and leads to nonequivalence of the protons in the ethyl and isobutyl derivatives. This does not occur for the *l*-borneol derivatives, since the borneol moiety cannot interact with the alkyl groups bound to the aluminum because of its orientation and rigidity.

Introduction

During the past several years a great deal of interest has been focused on the use of organometallic compounds in regio- and stereospecific organic synthesis.[1] Increasing emphasis has been placed on the transfer of optical activity from a transition-metal or a main-group-metal center to the substrate. Among the main-group metals studied, the modified aluminum hydride "ate" complexes, incorporating in them an optically active center (e.g., $LiAlH_2(OR)_2$, $LiAlH_2(O_2R)$; R = optically active group), have been found to be very attractive intermediates in enantio- and stereoselective organic syntheses.[2,3] Recently a few optically active organoaluminum compounds such as $EtAl(Cl)OR^*$[4] (OR^* = *l*-mentholate) have been proposed, but never isolated and characterized, as reaction intermediates in the enantioselective ortho hydroxyalkylation of phenols[5] and in asymmetric Diels–Alder reactions.[6] As a part of our investigations of the reactions of alkylaluminum compounds with protic organic substrates,[7] we report the synthesis and detailed spectroscopic investigations of optically active organoaluminum alkoxides derived from *l*-menthol and *l*-borneol and the first structural characterization of optically active organoaluminum alkoxides $[Me_2Al(\mu\text{-}l\text{-mentholate})]_2$, $[(i\text{-Bu})_2Al(\mu\text{-}l\text{-mentholate})]_2$, and $[Me_2Al(\mu\text{-}l\text{-borneolate})]_2$. We have also studied the temperature dependence of the ^1H NMR spectra of these derivatives and have determined that in the *l*-menthol derivatives hindered rotation occurs as a result of steric interaction between the menthol group and the alkyl substituents bound to the aluminum atom.

Experimental Section

General Data. All solvents were purified and dried by standard techniques.[8] Argon gas was purified by passing the argon through a series of columns containing Deox catalyst (Alfa), phosphorus pentoxide, and calcium sulfate. Aluminum alkyls

(1) Maruoka, K.; Banno, H.; Yamamoto, H. *J. Am. Chem. Soc.* **1990**, *112*, 7791 and references therein.
(2) Yamamoto, K.; Fukushima, H.; Nakazaki, M. *J. Chem. Soc., Chem. Commun.* **1984**, 1490.
(3) Noyori, R.; Tomino, I.; Tanimoto, Y.; Nishizawa, M. *J. Am. Chem. Soc.* **1984**, *106*, 6709.
(4) Hayakawa, Y.; Fueno, T.; Furukawa, J. *J. Polym. Sci., Part A-1* **1967**, *5*, 2099.
(5) Bigi, F.; Casiraghi, G.; Casnati, G.; Sartori, G.; Zetta, L. *J. Chem. Soc., Chem. Commun.* **1983**, 1210.
(6) Hashimoto, S.-I.; Komeshima, N.; Koga, K. *J. Chem. Soc., Chem. Commun.* **1979**, 437.
(7) Oliver, J. P.; Kumar, R. *Polyhedron* **1990**, *9*, 409.
(8) Shriver, D. F. *The Manipulation of Air-Sensitive Compounds*; McGraw-Hill: New York, 1969.

0276-7333/92/2311-0206$03.00/0